# A Simple Analytical Model of Periodic Coastal Upwelling

MIRKO ORLIĆ AND ZORAN PASARIĆ

*Andrija Mohorovičić Geophysical Institute, Faculty of Science, University of Zagreb, Zagreb, Croatia*

(Manuscript received 26 October 2010, in final form 10 February 2011)

ABSTRACT

An existing reduced-gravity model that reproduces the response of the coastal sea to alongshore wind forcing at subinertial frequencies is extended by allowing for cross-shore wind forcing and by considering superinertial frequencies. The obtained explicit solution shows that the wind-driven currents are predominantly controlled by friction and the Coriolis force at subinertial frequencies and by friction and local acceleration at superinertial frequencies. The effect of the coast is manifested by coastal-trapped variability at subinertial frequencies and baroclinic inertia–gravity waves propagating away from the coast at superinertial frequencies. The pycnocline oscillates at the coast not only at subinertial but also at superinertial frequencies, with the alongshore wind contributing more to the former and the cross-shore wind influencing more the latter. The oscillations are most pronounced when the periodic wind forcing is resonantly coupled to the local inertial oscillations (but only if the wind is not rotating counter to the inertial currents) and at near-zero frequencies (but not when the wind is purely cross-shore). These theoretical findings are related to recent observations of diurnal temperature oscillations in the near-shore water column.

## 1. Introduction

Coastal winds produce upwelling by forcing offshore transport in the surface layer, compensating onshore transport in the subsurface layer, and ascending motion close to the coast. Early studies of coastal upwelling focused on four eastern boundary currents and one western boundary current (the Canary Current off northwestern Africa, the Benguela Current off southwestern Africa, the California Current off western North America, the Peru Current off western South America, and the Somali Current off the Arabian Peninsula) and inspired the development of steady-state models (Smith 1968).

However, even at an early stage, it was recognized that the assumption of a steady state may not be generally applicable and that coastal upwelling often varies in time because of the variability of wind forcing. The first time scale to be recognized was seasonal, particularly in the Arabian Peninsula region, where upwelling is related to strong summer monsoon winds (Smith 1968). Subsequent investigations, enabled by the new technology of continuous current and temperature measurements, revealed some shorter time scales, including day to day (e.g., Smith 1981; Codispoti 1981) and diurnal (e.g., Halpern 1977; Rosenfeld 1988; Chen et al. 1996; Jarosz et al. 2007; Zhang et al. 2009), and pointed to several new regions where time-variable upwelling occurs. These investigations also stimulated an interest in simple conceptual models of coastal upwelling generated by periodic winds.

In all of the models, it was assumed that periodic wind stress acts on the sea in the vicinity of a straight coast. There were, however, numerous differences between the models, particularly in the way they considered stratification, a change of wind direction, and the frequency dependence of the forcing. As for the stratification, the sea was assumed to be homogeneous (Shaffer 1972; Rosenfeld 1988; Craig 1989), 1.5 layer (Cushman-Roisin 1994), two layer (Clancy et al. 1979; Wolanski 1986; Rippeth et al. 2002; Simpson et al. 2002), and continuously stratified (Dalu and Pielke 1990; Lerczak et al. 2001; Davies and Xing 2003; Zhang et al. 2010). The wind was either taken to blow cross-shore (Shaffer 1972; Craig 1989; Lerczak et al. 2001; Rippeth et al. 2002; Davies and Xing 2003), to blow alongshore (Wolanski 1986; Rosenfeld 1988; Cushman-Roisin 1994), to follow a circular path (Dalu and Pielke 1990; Simpson et al. 2002; Zhang et al. 2010), or to originate in a mesoscale meteorological model coupled to the oceanographic model (Clancy et al. 1979).

*Corresponding author address:* Mirko Orlić, Andrija Mohorovičić Geophysical Institute, Faculty of Science, University of Zagreb, Horvatovac 95, 10000 Zagreb, Croatia.
E-mail: orlic@irb.hr

DOI: 10.1175/JPO-D-10-05000.1

Most of the models considered the entire frequency range, but some (Clancy et al. 1979; Wolanski 1986; Rosenfeld 1988; Cushman-Roisin 1994) concentrated on subinertial frequencies.

The models revealed several interesting features of periodic coastal upwelling, in particular the difference between the subinertial and superinertial frequencies, with the former being dominated by coastal-trapped variability and the latter being dominated by waves radiating away from the coast. Moreover, the models showed that the response of the sea to periodic wind forcing is exceptionally strong at latitudes where local inertial oscillations could be resonantly excited. In the discussion of the model results, more attention was paid to oscillating currents than to varying density. Because some recent observations have rekindled an interest in the upwelling-related variations of temperature at the smallest diurnal time scales (Kaplan et al. 2003; Woodson et al. 2007), we aim in this note to present a simple, closed-form solution for periodic coastal upwelling and to discuss in particular how pycnocline variability depends on the type and the frequency of wind forcing.

The model selected for this purpose is the reduced-gravity model originally proposed by Cushman-Roisin (1994). It is the simplest model allowing for pycnocline variability driven by periodic winds at the coast, and it possesses the elegance expected from a good textbook model. In section 2, the model is extended by allowing not only for alongshore but also cross-shore wind forcing and by considering both the subinertial and superinertial frequencies. In section 3, the pycnocline oscillations provided by the model are discussed in some detail and are related to recent empirical findings.

## 2. The model

Here, we consider the reduced-gravity sea on the $f$ plane. The upper layer of average depth $H$ is placed over the motionless, infinitely deep lower layer. The sea is bounded by a vertical wall at $x = 0$ and occupies the positive-$x$ half plane. The cross-shore ($x$ direction) and the alongshore ($y$ direction) velocities are denoted by $u$ and $v$, respectively, and the displacement of the interface between the layers is denoted by $\eta$. In the absence of alongshore variations, the equations of motion and continuity are (e.g., Cushman-Roisin 1994)

$$\begin{aligned} \frac{\partial u}{\partial t} - fv &= g'\frac{\partial \eta}{\partial x} + \frac{\tau_x}{\rho_0 H}, \\ \frac{\partial v}{\partial t} + fu &= \frac{\tau_y}{\rho_0 H}, \quad \text{and} \\ H\frac{\partial u}{\partial x} - \frac{\partial \eta}{\partial t} &= 0. \end{aligned} \tag{1}$$

Here, $f$ is the Coriolis parameter, $\rho_0$ is the density of the lower layer, $g' = g\Delta\rho/\rho_0$ is the reduced gravity, and $\Delta\rho$ is the density difference between the two layers. Also, $\tau_x$ and $\tau_y$ are the components of the wind stress acting on the sea surface. Nonlinear terms are neglected. The boundary condition to be met at the vertical wall is

$$u(x = 0) = 0.$$

Far from the coast, the solution must remain bounded in magnitude.

In the present study, we are interested in periodic wind stress. Therefore, we use

$$\tau_x = A\sin(\omega t) \quad \text{and}$$

$$\tau_y = B\cos(\omega t),$$

meaning that the spatially constant wind rotates over time, following an elliptical, circular, or linear path. Parameter $A$ is taken to be nonnegative (offshore), whereas $B$ may be positive or negative, resulting in anticyclonic or cyclonic wind rotation, respectively. By varying magnitudes $A$ and $B$, we smoothly cover the two canonical cases: periodically varying alongshore wind ($A = 0$) and periodically varying cross-shore wind ($B = 0$).

For the fixed frequency $\omega > 0$ and $i^2 = -1$, periodic solutions are sought in the form $u(x, t) = u_0(x)\exp(i\omega t)$ and analogously for $v$ and $\eta$. Substitution into (1) leads to an ordinary differential equation

$$\frac{d^2u_0}{dx^2} - \frac{f^2 - \omega^2}{g'H}u_0 = -\frac{\omega A + fB}{\rho_0 g' H^2}, \tag{2}$$

whose solution $u_0$ must be bounded and must satisfy $u_0(x = 0) = 0$. Because the right-hand side is constant, (2) has a constant particular solution, which is easily found. The solution $u_0$ that is bounded and satisfies the boundary condition at the coast is found by utilizing the general solution of the homogeneous equation. Thereafter, functions $v_0$ and $\eta_0$ are obtained according to

$$\begin{aligned} v_0 &= \frac{1}{i\omega}\left(\frac{B}{\rho_0 H} - fu_0\right), \\ \eta_0 &= \frac{H}{i\omega}\frac{du_0}{dx}. \end{aligned}$$

By multiplying $u_0$, $v_0$, and $\eta_0$ with $\exp(i\omega t)$ and retaining only the real part, in the case $\omega < f$ the solution to (1) reads as follows:

$$u = \frac{R_a^2}{\rho_0 g' H^2}(\omega A + fB)(1 - e^{-(x/R_a)})\cos(\omega t),$$

$$v = -\frac{R_a^2}{\rho_0 g' H^2}\left[fA(1 - e^{-(x/R_a)}) + \omega B\left(1 - \frac{f^2}{\omega^2}e^{-(x/R_a)}\right)\right] \times \sin(\omega t), \quad \text{and}$$

$$\eta = \frac{R_a}{\rho_0 g' H}\left(A + \frac{fB}{\omega}\right)e^{-(x/R_a)}\sin(\omega t), \tag{3}$$

where

$$R_a = \sqrt{\frac{g'H}{f^2 - \omega^2}}.$$

In the case $\omega > f$ we get

$$u = -\frac{R_b^2}{\rho_0 g' H^2}(\omega A + fB)\left[\cos(\omega t) - \cos\left(-\frac{x}{R_b} + \omega t\right)\right],$$

$$v = \frac{R_b^2}{\rho_0 g' H^2}\left\{fA\left[\sin(\omega t) - \sin\left(-\frac{x}{R_b} + \omega t\right)\right] + \omega B\left[\sin(\omega t) - \frac{f^2}{\omega^2}\sin\left(-\frac{x}{R_b} + \omega t\right)\right]\right\}, \quad \text{and}$$

$$\eta = -\frac{R_b}{\rho_0 g' H}\left(A + \frac{fB}{\omega}\right)\cos\left(-\frac{x}{R_b} + \omega t\right), \tag{4}$$

where

$$R_b = \sqrt{\frac{g'H}{\omega^2 - f^2}}.$$

Obviously, solutions (3) and (4) also incorporate the case $f < 0$. What is important is the sign of $f$ as compared to the sign of $B$, meaning that the solution for the Southern Hemisphere is obtained from the respective Northern Hemisphere solution simply by reversing the signs of $B$ and $v$. However, in the discussion, we concentrate on the Northern Hemisphere.

## 3. Discussion

In solutions (3) and (4), there are terms that are spatially constant and terms that depend on $x$. The former represent the response of the unbounded sea to periodic wind forcing, and the latter document the effect of the coast. The influence of periodic wind on an unbounded sea strongly depends on the frequency of the forcing. It is obvious from (3) that, for very low subinertial frequencies, the current is directed to the right of the wind, oscillates in phase with it, and amounts to $(A, B)/(\rho_0 Hf)$: that is, it represents the classical Ekman drift. The primary balance is then between friction and the Coriolis force (Ekman 1905), with acceleration effects contributing at somewhat higher but still subinertial frequencies. As implied by (4) for very high superinertial frequencies, the current is directed down the wind causing it, lags the wind by a quarter period, and is equal to $(A, B)/(\rho_0 H\omega)$. In this case, the primary balance is between friction and local acceleration, with rotational effects creeping in at somewhat lower but still superinertial frequencies. It is noteworthy that Zöppritz (1878) has already studied wind-driven dynamics by balancing friction and local acceleration; however, he concentrated on vertically variable currents rather than transports and on laminar rather than turbulent viscosity.

As for the effect of the coast, it is also sensitively dependent on the frequency of the forcing. Solution (3) clearly shows that, at subinertial frequencies, the coast modifies the currents and supports the oscillations of the pycnocline with the variability being trapped at the coast within a distance of an order of $R_a$. The distance equals the internal radius of deformation for very low frequencies and becomes large when frequencies are close to the inertial frequency. Solution (4) makes it obvious that, at superinertial frequencies, the coast supports the generation of baroclinic inertia–gravity waves, which propagate outward at a phase speed equal to $\omega R_b$. The speed is equal to the speed of the baroclinic waves in nonrotating 1.5-layer sea for very high frequencies, and it increases at frequencies nearing the inertial frequency in accordance with the dispersion relation for internal inertia–gravity waves ($\omega^2 = f^2 + g'Hk^2$, where $k$ is the wavenumber).

Of special interest is the pycnocline variability at the coast, because it reflects periodic upwelling. To depict this variability, as implied by the third equations of (3) and (4), the following parameters are chosen: $\rho_0 = 1000$ kg m$^{-3}$, $\Delta\rho = 1.5$ kg m$^{-3}$, $H = 20$ m, and $g = 9.81$ m s$^{-2}$. Moreover, it is assumed that $A = \tau\cos\phi$ and $B = \tau\sin\phi$ with $\tau = 0.1$ N m$^{-2}$ so that wind forcing is simply parameterized and varies from alongshore ($\phi = -\pi/2$) via counterclockwise rotating to cross-shore ($\phi = 0$) and then via clockwise rotating back to alongshore ($\phi = \pi/2$). Figure 1 illustrates correspondence between the various types of wind forcing and parameter $\phi$, whereas Figs. 2 and 3 show the amplitude of pycnocline oscillations as a function of the normalized frequency $\omega/f$ and parameter $\phi$ for two latitudes (45° and 15°, respectively). The figures illustrate a pronounced response to the periodic wind forcing close to the inertial frequency, where the resonance occurs, except when the wind follows a circular path while rotating counterclockwise, and at very low frequencies, where the persistent wind supports large excursions of the pycnocline, except if it is directed purely cross-shore. In these two frequency bands,

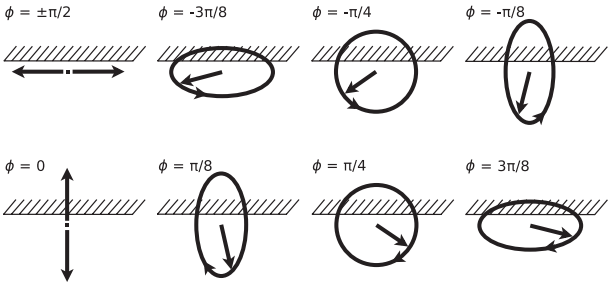


FIG. 1. Various types of wind forcing shown relative to the coast and their correspondence with parameter $\phi$. The wind is alongshore ($\phi = \pm\pi/2$); counterclockwise rotating ($-\pi/2 < \phi < 0$) following an elliptical or, in a special case, a circular path ($\phi = -\pi/4$); cross-shore ($\phi = 0$); and clockwise rotating ($0 < \phi < \pi/2$), again following an elliptical or, in the case $\phi = \pi/4$, a circular path.

the solution fails, signaling that the amplitude of the motion becomes so great that the assumption of linearity is no longer justified.

Subinertial variability is overall much larger than superinertial variability, with the alongshore wind contributing more to the former (the maximum at the lowest frequencies in Figs. 2 and 3 corresponds to $\phi = \pm\pi/2$) and the cross-shore wind contributing more to the latter (the maximum at the highest frequencies in Figs. 2 and 3 is positioned close to $\phi = 0$). This reflects the previously mentioned difference in the wind-driven currents, which are Ekman type and therefore directed to the right of the wind at subinertial frequencies, whereas they are Zöppritz like and consequently directed downwind at superinertial frequencies. Because the upwelling is supported by an offshore transport in the surface layer, the difference between the two dynamic regimes implies that the pycnocline is most efficiently pumped by the alongshore wind at subinertial frequencies and by the cross-shore wind at superinertial frequencies. Figures 2 and 3 also show that both subinertial and superinertial variability are enhanced in an equatorward direction when the stratification and wind forcing are fixed.

Several of these findings have already been obtained by previous modelers. For example, Dalu and Pielke (1990) pointed to coastal trapping at subinertial frequencies as opposed to offshore propagation at superinertial frequencies, Simpson et al. (2002) showed that resonance is not possible when the wind rotates counterclockwise following a circular path even if the frequency of rotation is equal to the local inertial frequency, and Zhang et al. (2010) analyzed in some detail the evolution of the current and density fields close to the coast at both subinertial and superinertial frequencies. What is novel in this work is a demonstration of the importance of cross-shore wind at superinertial frequencies

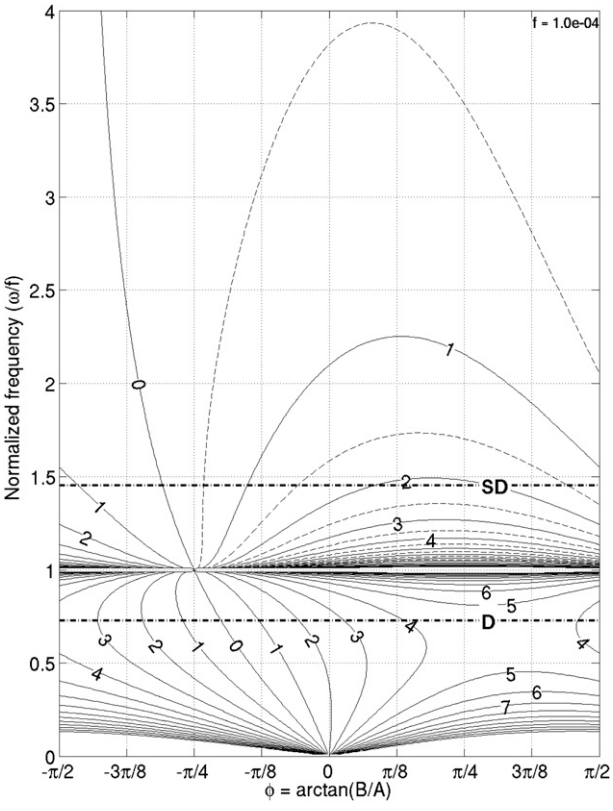


FIG. 2. The amplitude of the coastal pycnocline oscillations (in m) as a function of the frequency of wind forcing normalized by the inertial frequency and of the type of wind forcing determined by parameter $\phi$ (cf. Fig. 1). Dashed–dotted lines indicate diurnal (denoted as D) and semidiurnal (denoted as SD) frequencies. The Coriolis parameter corresponds to a 45° latitude, whereas all the other parameters used to prepare the figure are given in the text.

as opposed to the central role of alongshore wind at subinertial frequencies, the results obtained for the periodic wind following elliptical paths, and an explicit solution enabling the response of the stratified coastal sea to realistic wind forcing to be considered in the simplest possible terms.

The present model results may be related to recent observations of diurnal temperature oscillations in the near-shore water column. The model-to-data comparison could be only qualitative because, among other things, the model does not accommodate the finite bottom depth. Still, the exercise proves to be useful in at least two cases. Kaplan et al. (2003) analyzed time series collected along the coast of Chile above, at, and below the critical latitude. The authors showed that diurnal temperature oscillations are pronounced not only when they are subinertial but also when they are superinertial, which is in agreement with Figs. 2 and 3 and the equatorward intensification implied by the figures. This finding is different from the opinion occasionally encountered in the literature that

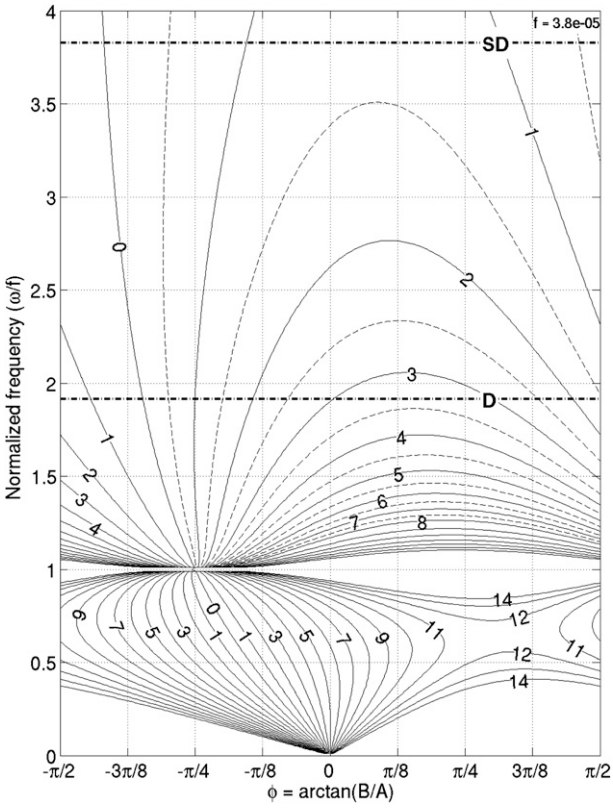


FIG. 3. As in Fig. 2, but for a 15° latitude.

upwelling occurs only when the frequency of the forcing is subinertial. It is also interesting that Kaplan et al. did not obtain a strong response at the critical latitude. As implied by solutions (3) and (4), resonance does not occur if the diurnal wind is rotating contrary to the inertial currents. Sea and land breezes may change the sense of rotation if they are influenced not only by the cross-shore air pressure gradient and the Coriolis force but also by the alongshore air pressure gradient (e.g., Kusuda and Alpert 1983); however, it is not known whether this occurs on the Chilean coast at the critical latitude. Another possible explanation for the lack of resonance is a change in the effective Coriolis constant due to the influence of background relative vorticity, a mechanism studied by Lerczak et al. (2001) but not included in the present model.

The observations of Woodson et al. (2007) on diurnal temperature variability in Monterey Bay at about 37°N are also interesting. They show that the variability is pronounced at the coast and the station positioned about 5 km off the coast but that it is reduced at a distance of about 10 km from the coast. Because the local internal radius of deformation may be estimated at about 4 km, whereas $R_a$ is approximately 2 times larger, the empirical finding apparently corresponds with solution (3), according to which the subinertial interface oscillations extend far from the coast when the basin is positioned close to the critical latitude.

*Acknowledgments.* We thank Dr. J. A. Barth and an anonymous reviewer for providing constructive comments on the manuscript. The work was supported by the Ministry of Science, Education and Sports of the Republic of Croatia (Grant 119-1193086-3085).

## REFERENCES

Chen, C., R. O. Reid, and W. D. Nowlin Jr., 1996: Near-inertial oscillations over the Texas-Louisiana shelf. *J. Geophys. Res.,* **101** (C2), 3509–3524.

Clancy, R. M., J. D. Thompson, H. E. Hurlburt, and J. D. Lee, 1979: Model of mesoscale air-sea interaction in a sea breeze-coastal upwelling regime. *Mon. Wea. Rev.,* **107,** 1476–1505.

Codispoti, L. A., 1981: Temporal nutrient variability in three different upwelling regions. *Coastal Upwelling,* F. A. Richards, Ed., Amer. Geophys. Union, 209–220.

Craig, P. D., 1989: A model of diurnally forced vertical current structure near 30° latitude. *Cont. Shelf Res.,* **9,** 965–980.

Cushman-Roisin, B., 1994: *Introduction to Geophysical Fluid Dynamics*. Prentice-Hall, 320 pp.

Dalu, G. A., and R. A. Pielke, 1990: An analytical study of the frictional response of coastal currents and upwelling to wind stress. *J. Geophys. Res.,* **95** (C2), 1523–1536.

Davies, A. M., and J. Xing, 2003: Processes influencing wind-induced current profiles in near coastal stratified regions. *Cont. Shelf Res.,* **23,** 1379–1400, doi:10.1016/S0278-4343(03)00119-5.

Ekman, V. W., 1905: On the influence of the earth's rotation on ocean-currents. *Ark. Mat. Astron. Fys.,* **2,** 1–52.

Halpern, D., 1977: Description of wind and of upper ocean current and temperature variations on the continental shelf off northwest Africa during March and April 1974. *J. Phys. Oceanogr.,* **7,** 422–430.

Jarosz, E., Z. R. Hallock, and W. J. Teague, 2007: Near-inertial currents in the DeSoto Canyon region. *Cont. Shelf Res.,* **27,** 2407–2426.

Kaplan, D. M., J. L. Largier, S. Navarrete, R. Guiñez, and J. C. Castilla, 2003: Large diurnal temperature fluctuations in the nearshore water column. *Estuarine Coastal Shelf Sci.,* **57,** 385–398, doi:10.1016/S0272-7714(02)00363-3.

Kusuda, M., and P. Alpert, 1983: Anti-clockwise rotation of the wind hodograph. Part I: Theoretical study. *J. Atmos. Sci.,* **40,** 487–499.

Lerczak, J. A., M. C. Hendershott, and C. D. Winant, 2001: Observations and modeling of coastal internal waves driven by a diurnal sea breeze. *J. Geophys. Res.,* **106** (C9), 19 715–19 729.

Rippeth, T. P., J. H. Simpson, R. J. Player, and M. Garcia, 2002: Current oscillations in the diurnal-inertial band on the Catalonian shelf in spring. *Cont. Shelf Res.,* **22,** 247–265.

Rosenfeld, L. K., 1988: Diurnal period wind stress and current fluctuations over the continental shelf off Northern California. *J. Geophys. Res.,* **93** (C3), 2257–2276.

Shaffer, G., 1972: A theory of time-dependent upwelling induced by a spatially- and temporally-varying wind with emphasis on the effects of a seabreeze-landbreeze cycle. *Kiel. Meeresforsch.,* **28,** 139–161.

Simpson, J. H., P. Hyder, T. P. Rippeth, and I. M. Lucas, 2002: Forced oscillations near the critical latitude for diurnal-inertial resonance. *J. Phys. Oceanogr.,* **32,** 177–187.

Smith, R. L., 1968: Upwelling. *Oceanography and Marine Biology—An Annual Review,* Vol. 6, H. Barnes, Ed., George Allen and Unwin Ltd., 11–46.

——, 1981: A comparison of the structure and variability of the flow field in three coastal upwelling regions: Oregon, Northwest Africa, and Peru. *Coastal Upwelling,* F. A. Richards, Ed., American Geophysical Union, 107–118.

Wolanski, E., 1986: A simple analytical model of low-frequency wind-driven upwelling on a continental slope. *J. Phys. Oceanogr.,* **16,** 1694–1702.

Woodson, C. B., and Coauthors, 2007: Local diurnal upwelling driven by sea breezes in northern Monterey Bay. *Cont. Shelf Res.,* **27,** 2289–2302, doi:10.1016/j.csr.2007.05.014.

Zhang, X., S. F. DiMarco, D. C. Smith, M. K. Howard, A. E. Jochens, and R. D. Hetland, 2009: Near-resonant ocean response to sea breeze on a stratified continental shelf. *J. Phys. Oceanogr.,* **39,** 2137–2155.

——, D. C. Smith, S. F. DiMarco, and R. D. Hetland, 2010: A numerical study of sea-breeze-driven ocean Poincare wave propagation and mixing near the critical latitude. *J. Phys. Oceanogr.,* **40,** 48–66.

Zöppritz, K. J., 1878: Hydrodynamische Probleme in Beziehung zur Theorie der Meeresströmungen. *Ann. Phys. Chem.,* **238,** 582–607.